F. Méot, DAPNIA & IN2P3
G. Rees, RAL

NuFact muon storage ring : study of a design based on solenoid focusing decay straights

Contents

1 Ring geometry and parameters

Table 1 : Muon storage ring parameters.

Energy / Rigidity	(GeV / T.m)	20 / 67
Circumference	(m)	1170.764
Requested transverse acceptance	(π cm, norm.)	3
Requested $\delta p/p$ acceptance	(%)	±1
ν_x/ν_z *(present study)*		10.79 / 11.15
ξ_x/ξ_z		-14.3 / -14.9
Arcs		
10-cell arcs (2) :		
Length	(m)	78
Deviation	(deg)	96.73
Phase advance (μ_x/μ_z)	(2π)	2 / 2
ξ_x/ξ_z		-2.01 / -2.27
16-cell arc (1) :		
Length	(m)	124.8
Deviation	(deg)	154.766
Phase advance (μ_x/μ_z)	(2π)	3.2 / 3.2
ξ_x/ξ_z		-3.21 / -3.60
Arc cell :		
Length	(m)	7.8
Phase advance (μ_x/μ_z)	(deg)	72
ξ_x/ξ_z		
$\beta_{x,z}$ max	m	12.6
D_x max	m	1.08
Arc cell combined function dipole :		
Length	(m)	1.25
Deviation	(deg)	4.836
Curvature	(1/m)	0.337647
Foc. strength	(m^{-2})	±0.16

Production Straight		
Length	(m)	126
Number of solenoids	(/straight)	8
Solenoid field, length	(T, m)	4, 4
Phase advance (μ_x/μ_z)	(2π)	0.5 / 0.5
ξ_x/ξ_z		
$\beta_{x,z}$ max	(m)	100
Tuning/Collimation/RF straight Straight		
Length	(m)	148.364
Quad. strengths	(m^{-2})	< 0.11
Quad. lengths	(m)	110, 200, 300, 340
Phase advance (μ_x/μ_z)	(2π)	1.62 / 2.05
ξ_x/ξ_z		
$\beta_{x/z}$ max	(m)	103 / 58
D_x max	(m)	0.7
Matching sections		
Phase advance (μ_x/μ_z)	(2π)	0.97 / 0.9
ξ_x/ξ_z		

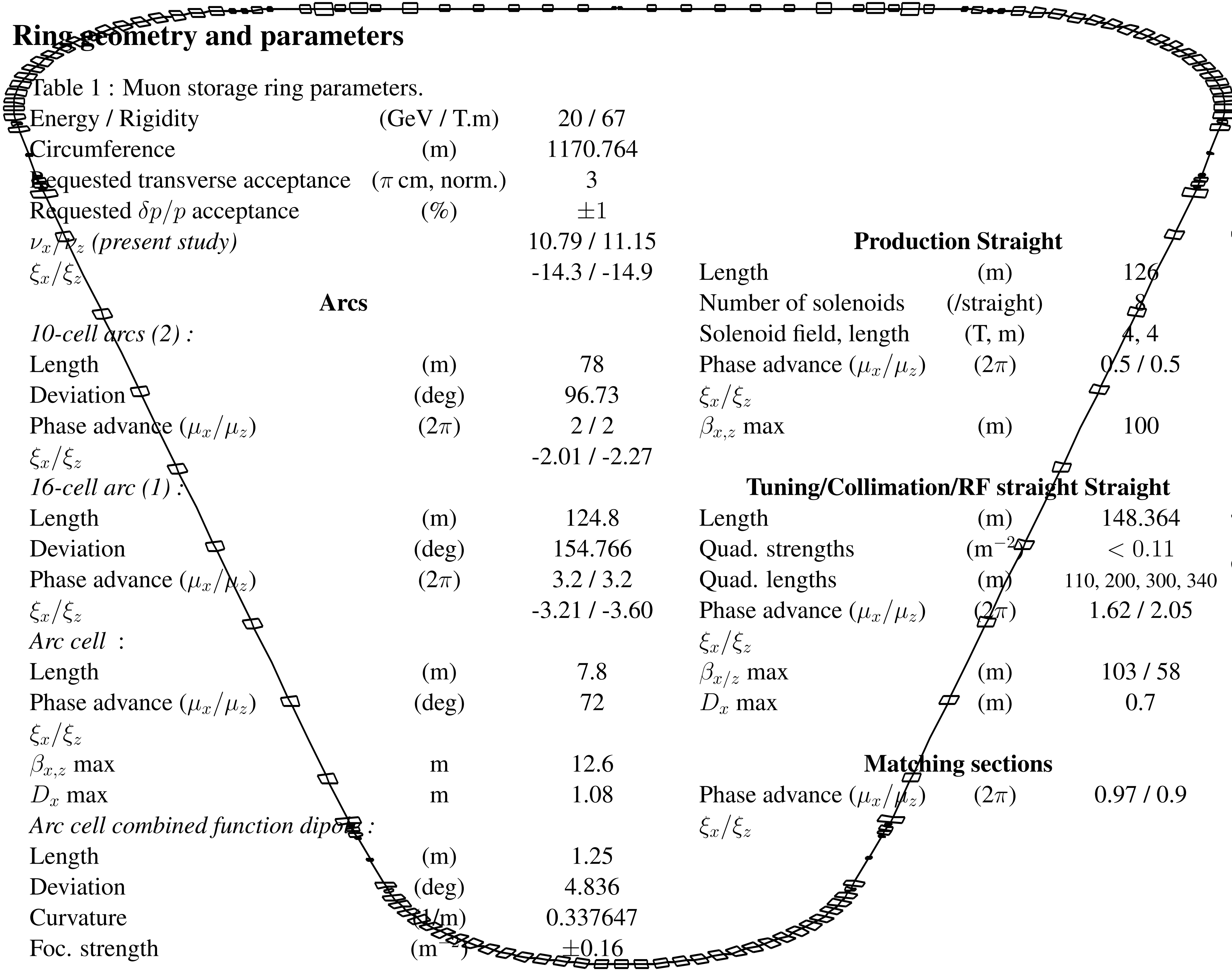

2 Building-up ray-tracing data

2.1 Arcs

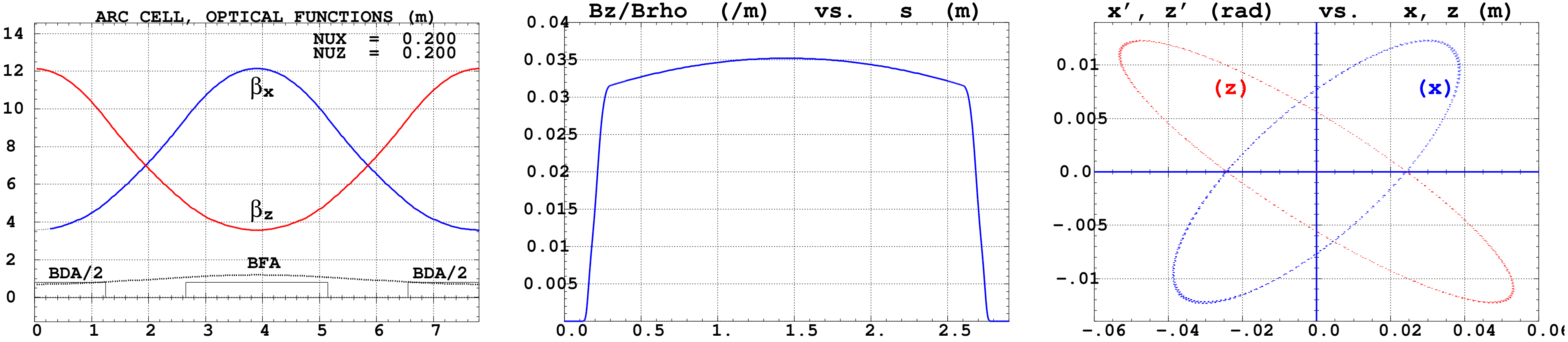

Figure 1: **Left : arc cell, optical functions and periodic dispersion.**
Middle : typical $B/B\rho$ at traversal of BFA-type combined function dipole, including fringe fields.
Right : horizontal and vertical phase space motion of a single particle, 10^5 passes, as observed at ends of arc cell. Particle launched on $\epsilon_x = \epsilon_z = 6\ \pi$cm.

Optics ingredients :

Magnet		type	length	$1/\rho$ (m^{-1})	K_1 (m^{-2})	angle (rad)	shift (10^{-2}m)
BFA	*Matrix method*	sbend	2.50	0.0337647	0.1580318	0.0844117	0
	Ray-tracing	sbend	2.50	id.	0.15917403	id.	1.78275
BDA	*Matrix method*	sbend	2.50	0.0337647	-0.1592295	0.0844117	0
	Ray-tracing	sbend	2.50	id.	-0.15817843	id.	1.72389

Chromaticity : $\xi_y \approx -\int \beta_y K_y ds \,/\, 4\pi \approx -N_Q(\beta_y|_{max} - \beta_y|_{min}) K_y L \,/\, 4\pi \Rightarrow \xi_x \approx \xi_z \approx -N_Q \times 2.2 \approx -8$

2.2 Solenoid straight

Ratio of divergences of the 20 GeV muon and the neutrino beam is set at 0.1 for an assumed (possibly incorrectly) muon, normalized, r.m.s. emittance of 4800 π mm mr.

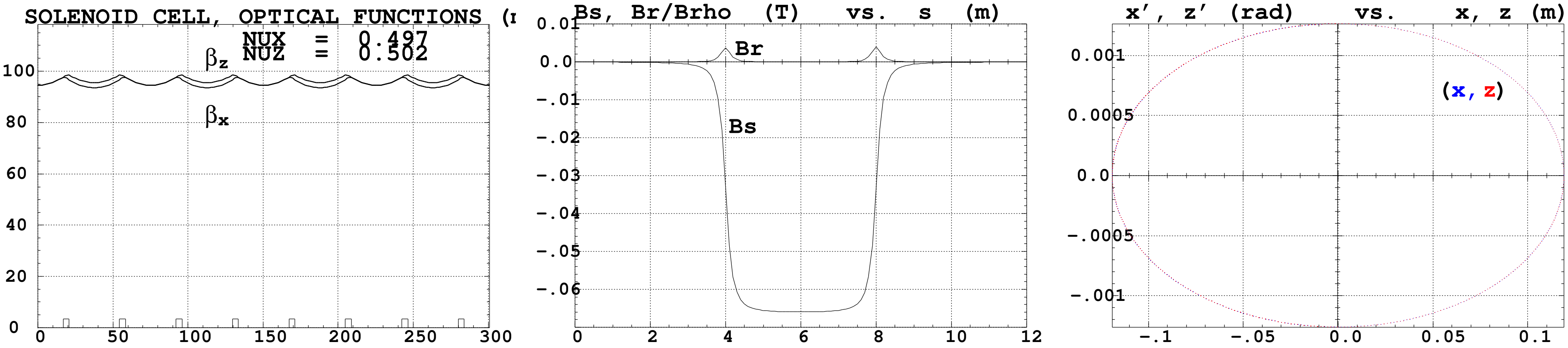

Figure 2: **Left : optical functions in the solenoid straight.**
Middle : typical field components at traversal of a solenoid, off-axis. 4 m fringe field extents are accounted for.
Right : horizontal and vertical (superimposed) phase space motion of a single particle, stepwise tracked over 2000 passes through the solenoid straight, observed at the straight end. Particle launched on $\epsilon_x/\pi = \epsilon_z/\pi = 3\,\pi$cm invariants, the phase advance is $0.4976 \times 2\pi$ per pass. An ellipse fitting yields $\beta_x = \beta_z = 94.4$ m, $\alpha \approx 0$. The integration step size is 1 cm.

Optics ingredients :

	length (m)	$B_s/2B\rho$ (m^{-1})	fall-off extent (m)	$\Omega = B_sL/2B\rho$ (rad)
Matrix method	4	0.0318503	0	
Ray − tracing	4	0.0331322	4	

———

2.3 Tuning/Collimation/RF straight

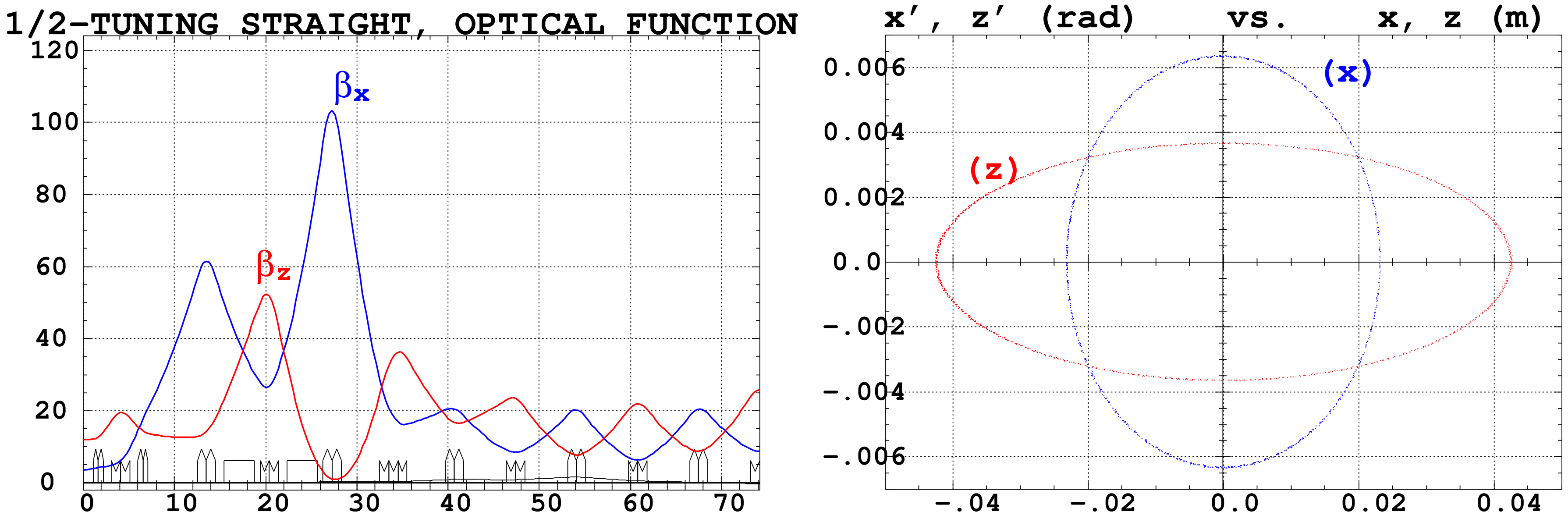

Figure 3: **Left : optical functions in half the collimation/tuning/RF straight (from arc to straight center).**
Right : a 10^4-pass tracking of a single particle launched with $\epsilon_x = \epsilon_z = 3\pi$ cm (norm.), through the collimation straight ; x and z phase space motion are observed at the straight end ; this yields $\beta_x = 3.65$ m, $\beta_z = 11.60$ m, $\alpha_{x,z} \approx 0$; integration step size in quadrupole fringe field and body regions are respectively about 0.5 cm and 5 cm.

2.4 Full ring

- **Beam envelopes**

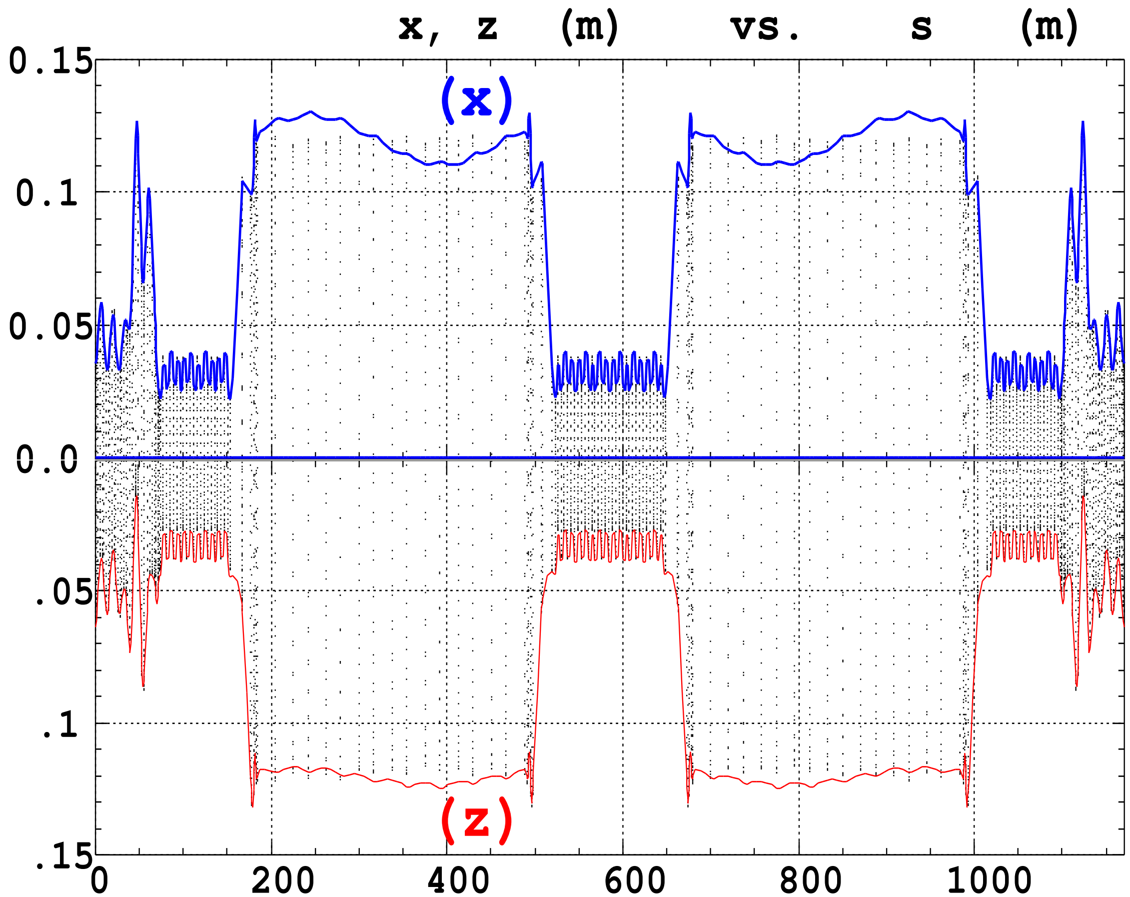

Figure 4: **Transverse positions, inside all optical elements, of 50 particles starting with coordinates evenly spread on $\beta\gamma\epsilon_{x,z} = 3\,\pi$ cm, together, for comparison with the envelopes obtained from regular matrix computation for comparison (solid lines).**

Full ring

- **Closed orbits**

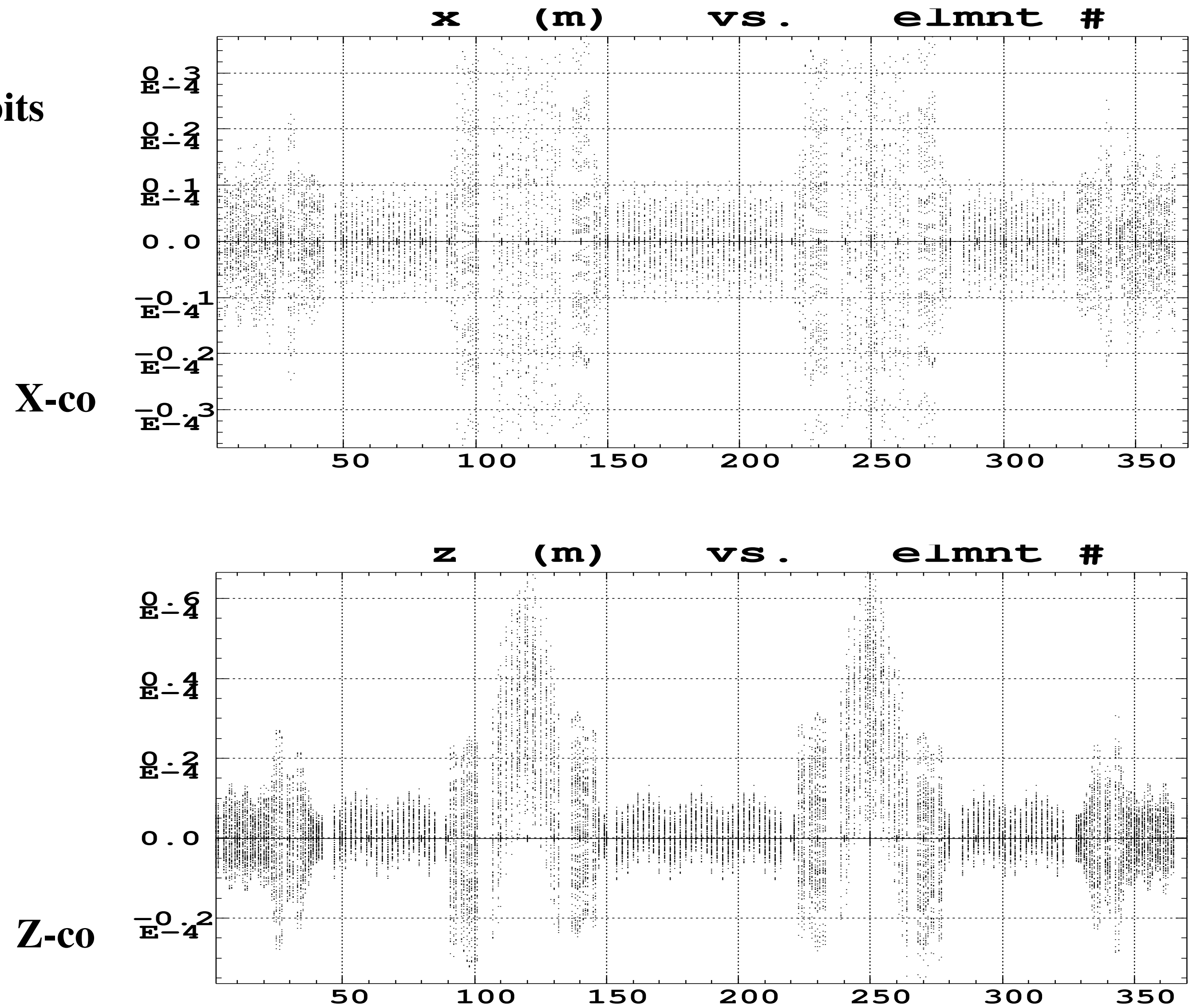

Figure 5: **Residual geometrical closed orbits.**

Full ring

- **Momentum dispersion**

Dx

Dz

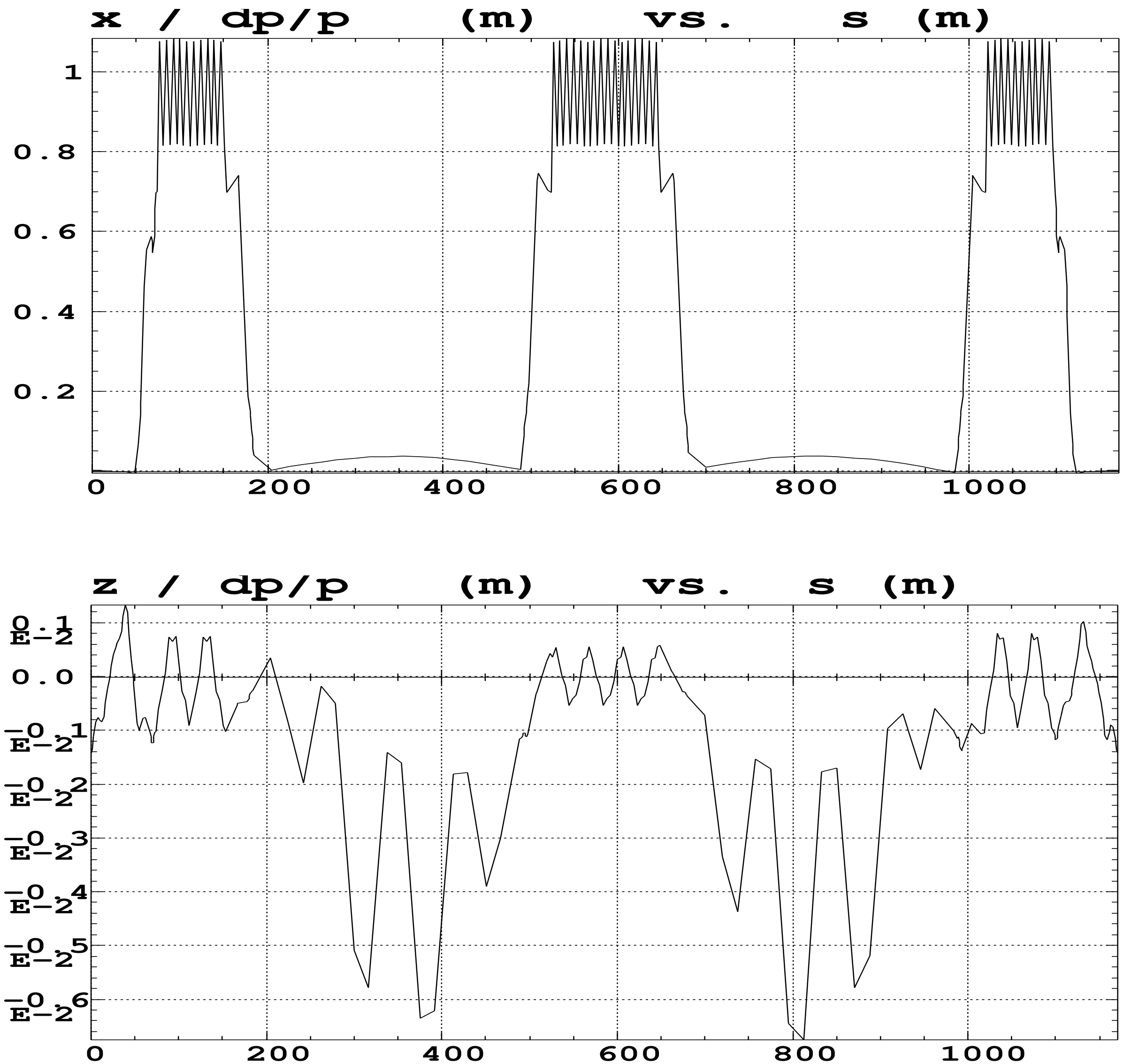

Figure 6: **Chromatic closed orbits.**

2.5 Large amplitude tracking, preliminary tests

A rapid idea of expectable acceptances. Clearly satisfactory at that stage.

- **Case of purely 2D initial beam coordiantes, maximum stable amplitudes :**

Maximum stable starting invariant (normalized)	induced emittance	corresponding tunes ν_x/ν_z
$\epsilon_x/\pi = 2.64 \times 3\,\pi$cm	$\epsilon_z/\pi = 0.01 \times 3\,\pi$cm	0.799 / 0.182
$\epsilon_z/\pi = 2.63 \times 3\,\pi$cm	$\epsilon_x/\pi = 0.03 \times 3\,\pi$cm	0.825 / 0.155

- **Case of $\delta p/p \neq 0$, maximum stable amplitudes affected by $\delta p/p$ in the absence of chromaticity corrections :**

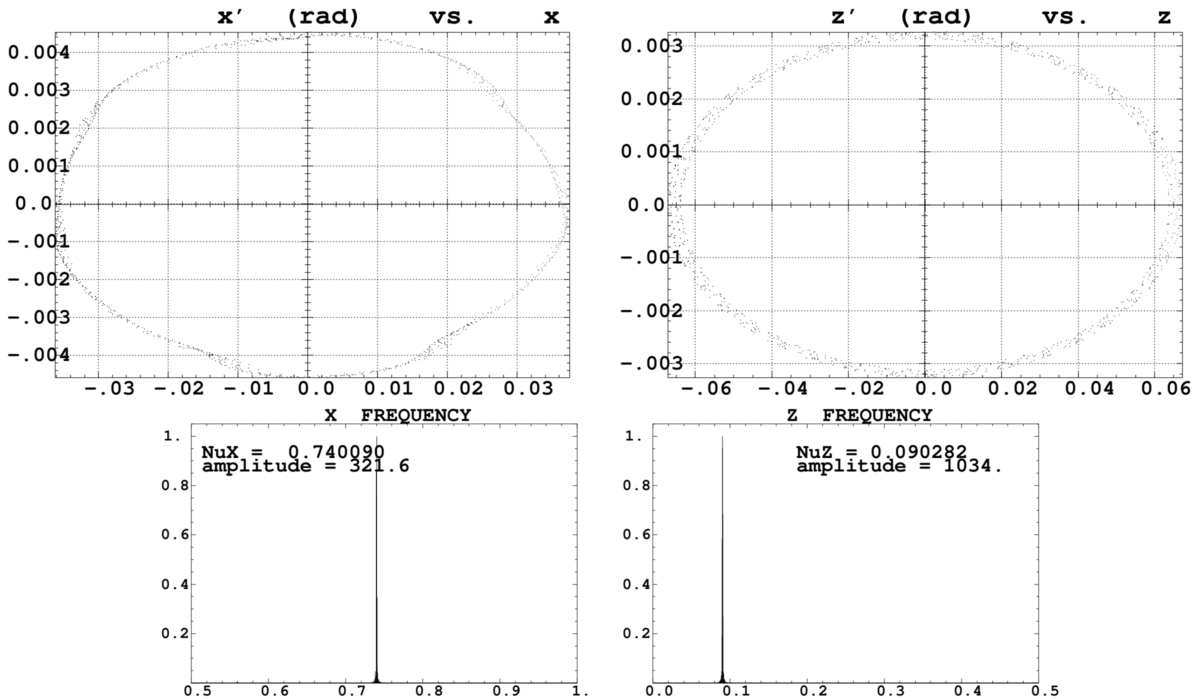

Figure 7: **Top : particle launched on $\epsilon_x = \epsilon_z = 3.6\,\pi$ cm invariants and with $\delta p/p = 0.5$%. 1000 turns in the ring. Bottom : corresponding spectra, victim of momentum detuning, featuring $\Delta\nu_{x,z} = \xi_{x,z}\delta p/p$, with $\xi_{x,z} \approx -15$.**

3 Tracking, linear machine

3.1 Large amplitude tests

Series of test in order to control the large amplitude behavior, both of the tracking method, and of the ring itself.
Investigations limited at this stage to $\epsilon_x/\pi = 3\,\pi$cm, $\epsilon_z/\pi = 3\,\pi$cm, $\delta p/p = \pm 1\%$.

Initial conditions used in these tests :

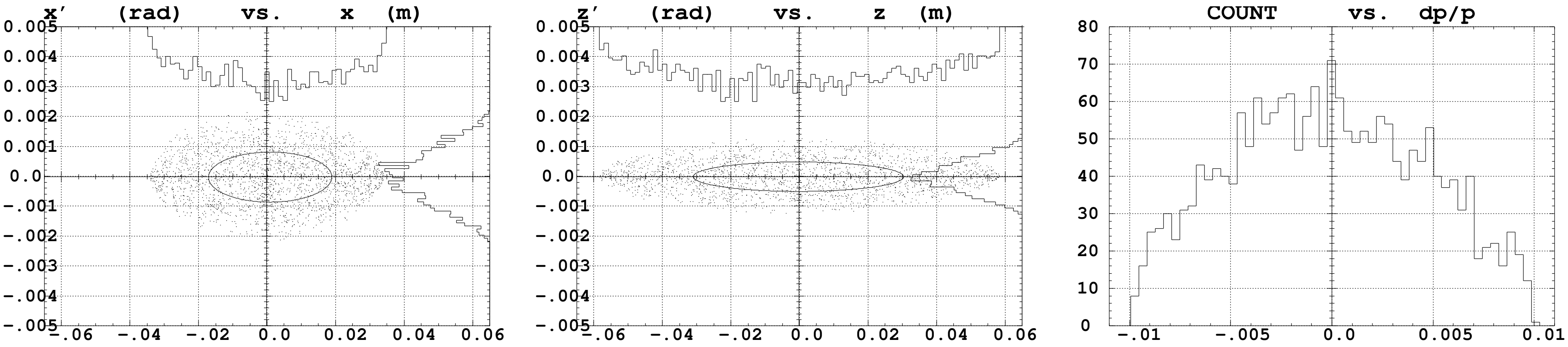

Figure 9: $\epsilon_x/\pi = 3\,\pi$**cm,** $\epsilon_z/\pi = 3\,\pi$**cm,** $\delta p/p = \pm 1\%$**.**

Preliminary tests on motion, 4-D + $\delta p/p$ initial conditions

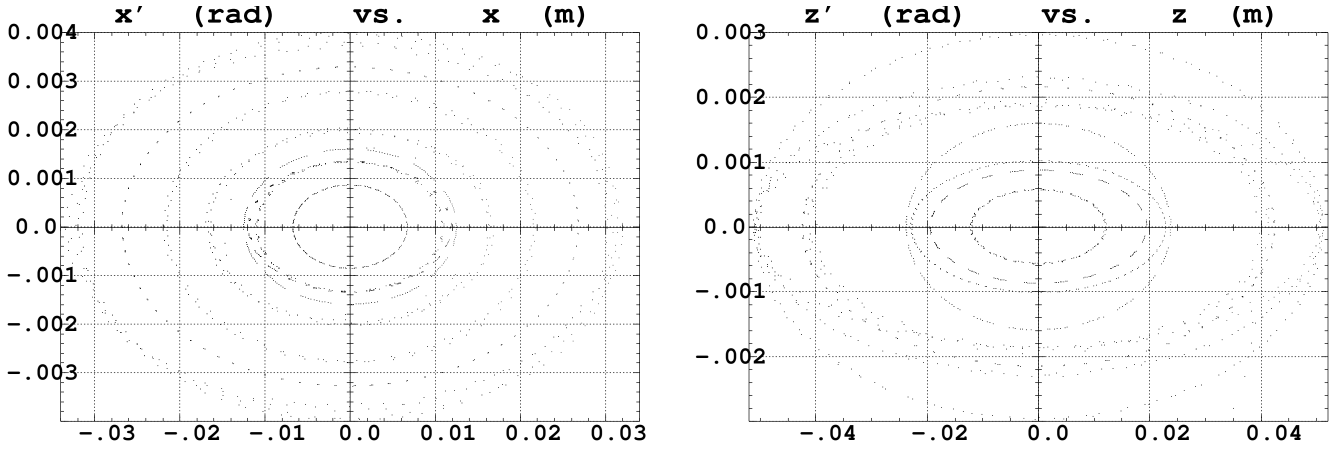

Figure 10: **Sample trajectories, (i) horizontal motion, (ii) vertical motion. Visible effect of chromaticity, $d\beta/\beta\ /\ \delta p/p$.**

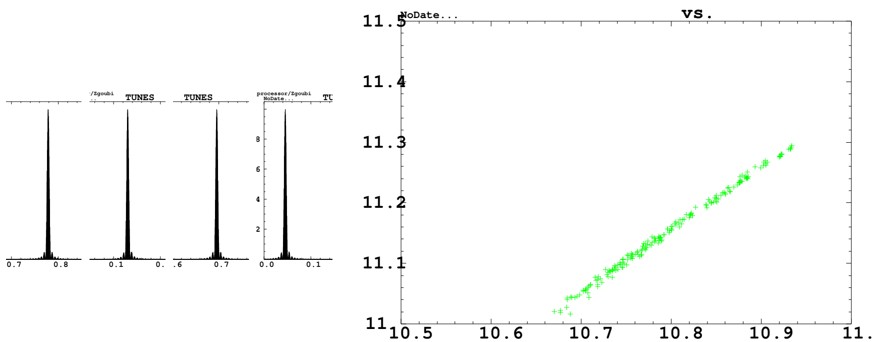

Figure 11: **(i) Sample spectra, all with single peak $\Rightarrow$ negligible coupling.
(ii) Tune diagram footprint, 200 particles features $\Delta\nu_{x,z} = \xi_{x,z}\delta p/p$.**

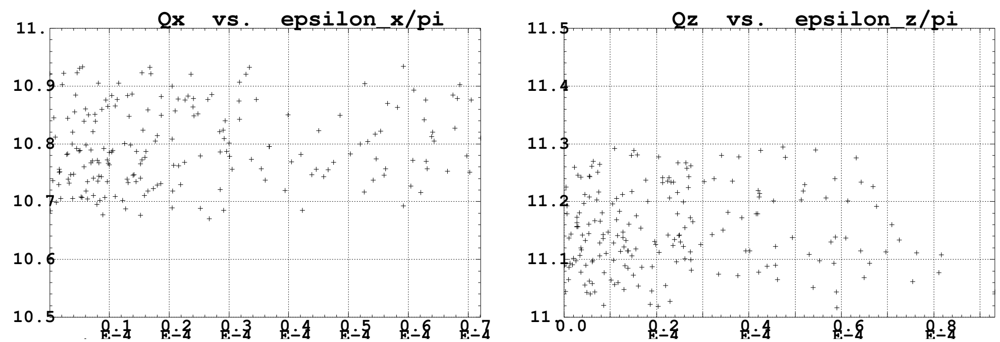

Figure 12: **No pronounced amplitude detuning (linear machine).
(i) ν_x as a function of ϵ_x/π.
(ii) ν_z as a function of ϵ_z/π.**

3.2 Transmission, 4-D + $\delta p/p$

3.2.1 Initial conditions, 2000 particles 1000 turns : $\epsilon_x = \epsilon_z = 3\,\pi$ cm (norm.), $\delta p/p = \pm 1\%$.

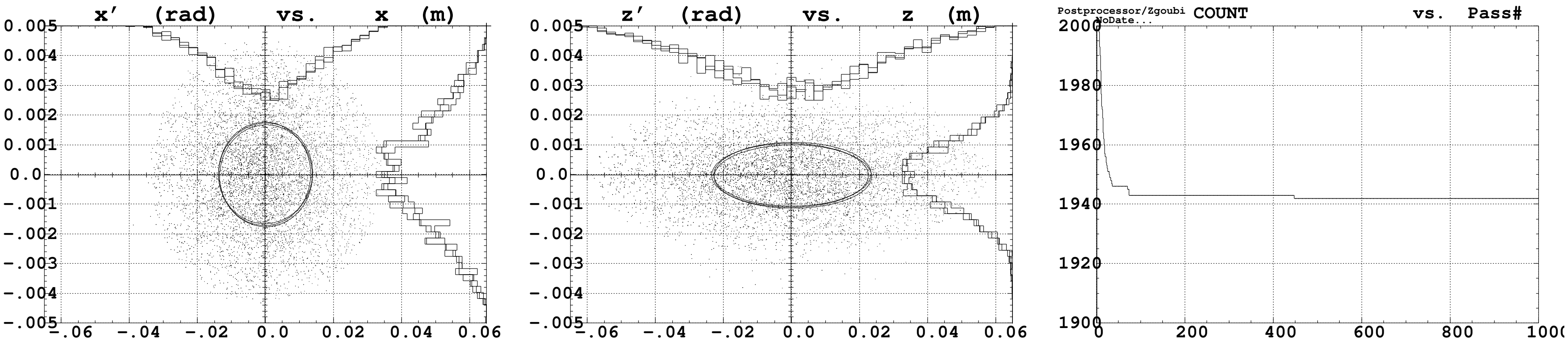

Figure 13: **Left and middle : a superposition of (resp. H and V) phase spaces and projected densities at turns # 100, 500 and 1000 ; the emittance and desnities practically do not change, meaning absence of sensible (numerical or real) diffusion effect.**
Right : number of particles transmitted vs turn number.

Transmission is 1942/2000 particles, despite non-corrected chromaticity.

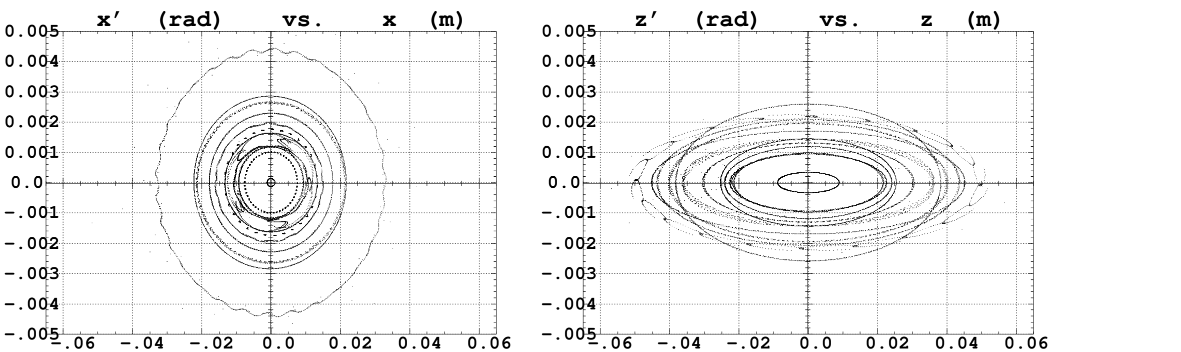

Figure 14: **Sample multiturn tracking, shows the good behavior of numerical integration.**

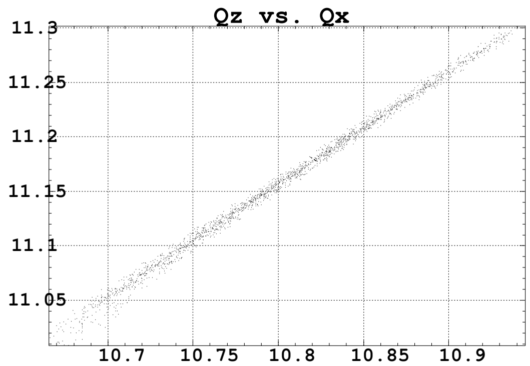

Figure 15: **Beam footprint in the tune diagram, with extent $\Delta\nu_{x,z} \approx -15\,\delta p/p$.**

3.2.2 Initial conditions, 10^4 particles, 1000 turns : $\epsilon_x = \epsilon_z = 6\,\pi$ cm (norm.), $\delta p/p = \pm 4\%$

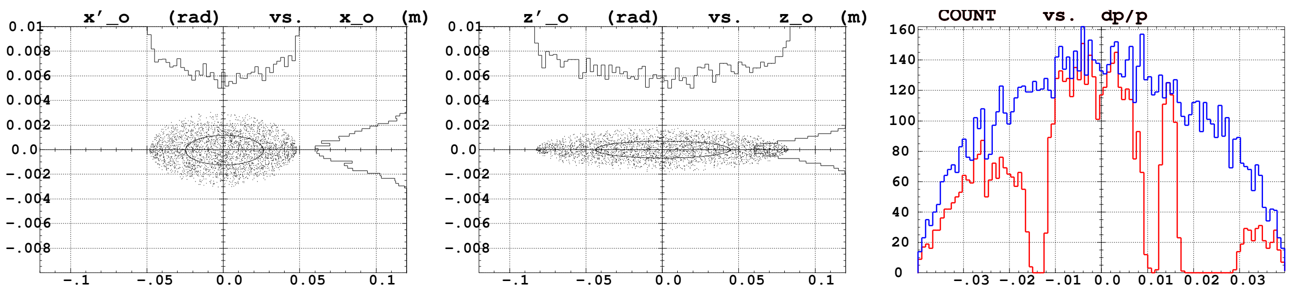

Figure 16: **Initial conditions, and transmitted momentum density (red histogram on the right).**

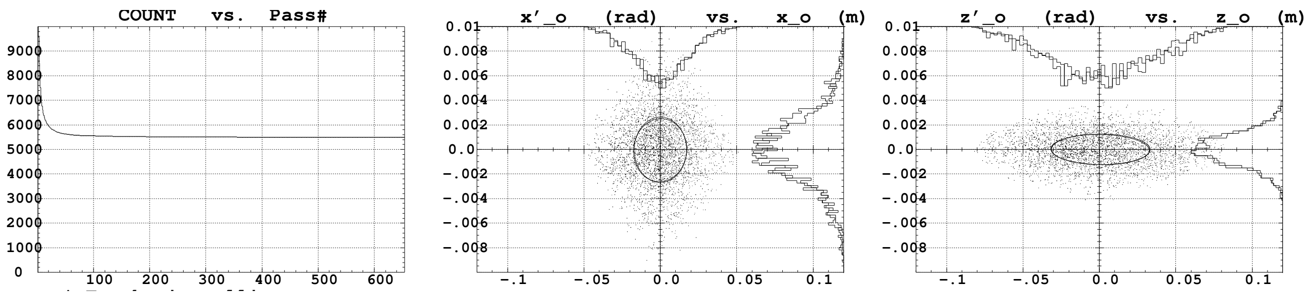

Figure 17: **Left : transmission.**
Middle and right : phase spaces and projected densities at turns # 300 and 650 → absence of sensible (numerical or real) diffusion effect.

Transmission is 5500/10000 particles, beam through : $\left\{ \begin{array}{l} \epsilon_x \approx \epsilon_z \approx 6\,\pi\ cm \\ \delta p/p \in [-1.2, 1]\% \end{array} \right.$.

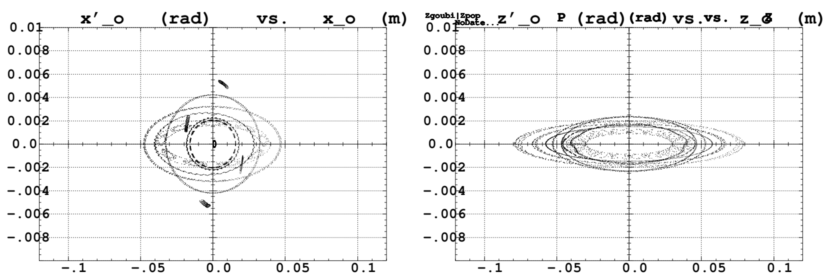

Figure 18: **Sample multiturn tracking, shows good behavior of numerical integration.**

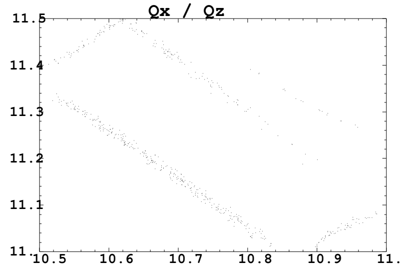

Figure 19: **Tune diagram, with extent due to chromaticity and coupling.**

4 Tracking, chromaticity compensated with sextupoles in arc bends

• Note : effects on c.o. of introduction of sextupoles in CF dipoles are not corrected (up to 2 mm in H plane)). Feed-down to tunes not corrected either.

- **Initial conditions, 10^3 particles, 1000 turns :** $\epsilon_x = \epsilon_z = 6\,\pi$ **cm (norm.),** $\delta p/p = \pm 4\%$

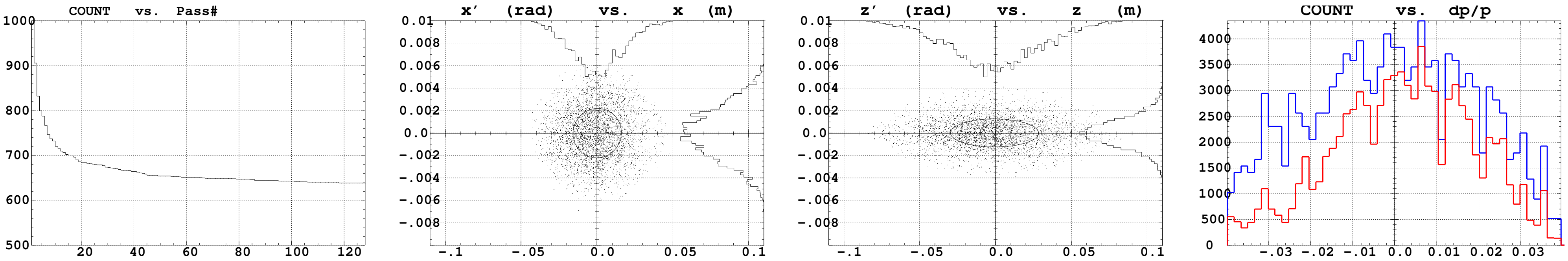

Figure 20: **Left : transmission.**
Middle two : phase spaces and densities at turns # 300 and 650 → no sensible (numerical or real) diffusion effect.
Right : Momentum densities, initial (blue) and transmitted (red).

Transmission is 630/1000 particles, beam through : $\left\{ \begin{array}{l} \epsilon_x \approx 4.6, \epsilon_z \approx 4.4\,\pi\, cm \\ \delta p/p \in [-4, +4]\% \end{array} \right.$.

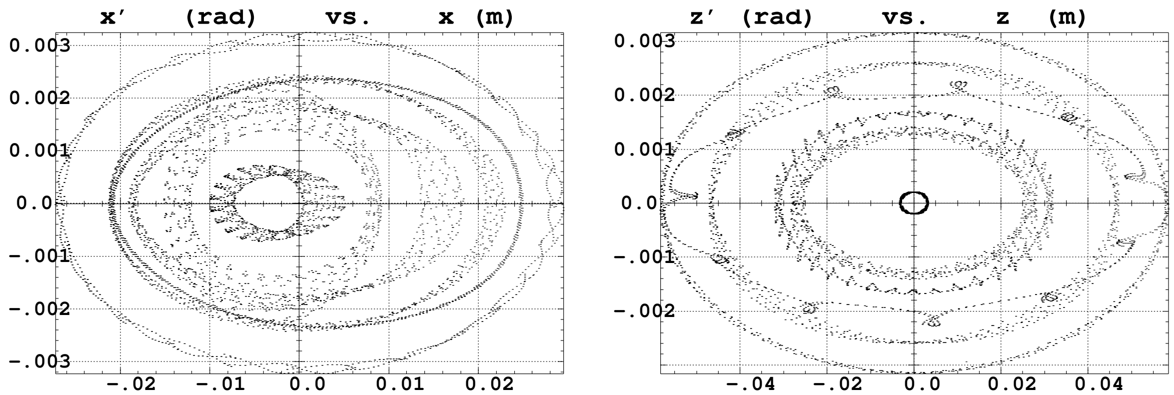

Figure 21: **Sample multiturn tracking. Shows good behavior of the numerical integration (no obvious non-symplectic behavior).**

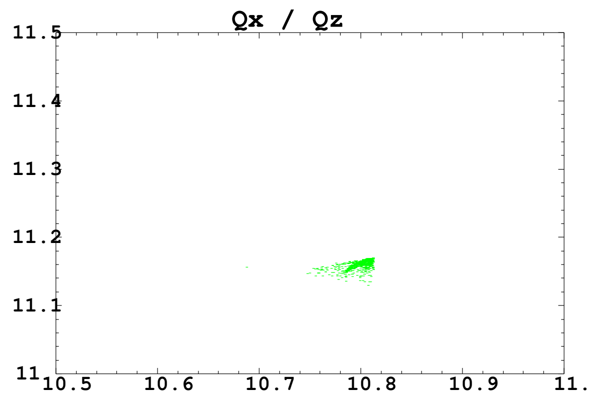

Figure 22: **Tune diagram, with extent due to chromaticity and coupling.**

ISS-NuFact, RAL, April 21-28, 2006. Muon decay ring. FM, GR

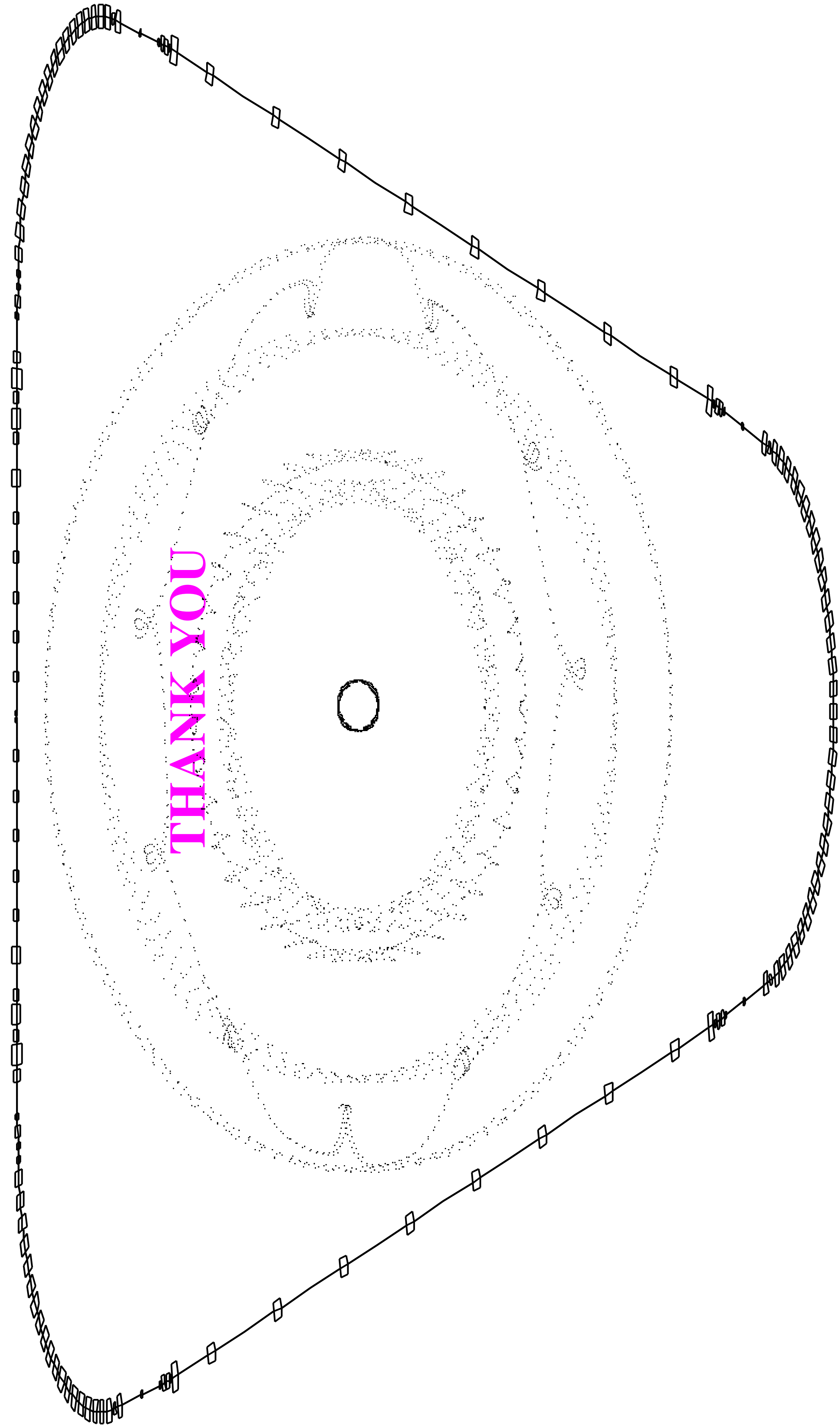

References

[1] G. Rees, Stormu20 (20 GeV, $\mu+$ and $\mu-$, Isosceles Triangle, Storage Rings.), private communication, Jan. 2006.

[2] F. Méot, The ray-tracing code Zgoubi, NIM A 427 (1999) 353-356.

[3] The BETA code, J. Payet, F. Méot, et *als.*, CEA/DAPNIA, Saclay.

[4] H. Grote, F. C. Iselin, The MAD Program, User's Reference Manual, CERN/SL/90-13 (AP) (Rev. 5), CERN, 29 April 1996.

[5] F. Méot, A. París, Concerning effects of fringe fields and longitudinal distribution of b_{10} in LHC low-β regions, Report FERMILAB-TM-2017, February 2, 1998.
F. Méot, On the effects of fringe fields in the LHC ring, Part. acc., 1996, Vol. 55, pp.[329-338]/83-92.
F. Méot, On the effects of fringe fields in the recycler ring, Report FERMILAB-TM-2016, April 15, 1997.

[6] G. Leleux, Compléments sur la physique des accélérateurs, DEA de Physique et Technologie des Grands Instruments, rapport CEA/DSM/LNS/86-101, CEA, Saclay (1986).

[7] H.A. Enge, Deflecting magnets, in *Focusing of charged particles*, volume 2, A. Septier ed., Academic Press, New-York and London (1967).

[8] G. Leleux, Influence of quadrupole fringe fields on wave numbers, Tech. report 6-67/GL-FB, LAL, Orsay (2 Feb. 1967).